

## HERMIONE, EVOLUTION OF A Te-BEARING EPITHERMAL MINERALIZATION, ARGOLIS, HELLAS

Tombros S.<sup>1</sup>, and St. Seymour K.<sup>1,2</sup>

<sup>1</sup> Department of Geology, Laboratory of Ore Deposits and Volcanology, University of Patras, 265.00, Patras, Hellas, [tompros@mailbox.gr](mailto:tompros@mailbox.gr), [kstseymr@upatras.gr](mailto:kstseymr@upatras.gr)

<sup>2</sup> Department of Geography, Concordia University, Montreal, Canada, [kstseymr@upatras.gr](mailto:kstseymr@upatras.gr)

### Abstract

The Cu-Te-bearing pyrite deposits of Hermione, Argolis are hosted in Miocenic ophiolites. The ophiolites are overlain by a shale-sandstone formation with intercalations of limestones and manganeseiferous sedimentary rocks. The ore deposits form irregular lenticular or stratiform ore bodies, and veins. These ore bodies are related to volcanic activity in an arc-related rift at the margins of a palaeocontinent. Late N- to NNE-trending, sinistral, milky quartz-pyrite-calcite veins cut the host ophiolites. Alteration haloes of quartz-calcite, albite-sericite-chlorite, and chalcedony-epidote-clay minerals are developed in the lavas as concentric shells, or as envelopes that parallel the quartz veins. The tellurium-bearing mineralization is developed in two successive stages, characterized by the assemblages: pyrite-(pyrrhotite)-magnetite-chalcopyrite-sphalerite (Stage I) and galena-sphalerite-freibergite-marcasite-chalcocite (Stage II), followed by a supergene stage. The cobaltiferous pyrite-chalcopyrite geothermometer defined two ranges of last-equilibration temperatures: 220° to 250°C for Stage I, and 120° to 195°C for Stage II. The calculated  $\delta^{18}\text{O}$  and  $\delta\text{D}$  compositions of the mineralizing fluids, at 200° and 250°C, reflect the dominance of a magmatic component. The calculated  $\delta^{34}\text{S}_{\text{H}_2\text{S}}$  fluid values reveal a magmatic source for the sulphur, with minor contribution from submarine sediments, whereas tellurium is proposed to be derived from a mafic-ultramafic source.

**Key words:** Tellurium-bearing cupriferous pyrite, ores, ophiolites, Miocene arc-related rift, Hermione, Argolis.

### Περίληψη

Τα κοιτάσματα Cu-Te σιδηροπυρίτη της Ερμιόνης, Αργολίδας φιλοξενούνται σε οφιόλιθους Μειοκαινικής ηλικίας. Οι οφιόλιθοι υπόκεινται σε έναν άργιλοψαμμιτικό σχηματισμό με ενδιαστρώσεις ασβεστολίθων και μαγνητιούχων ιζημάτων. Τα κοιτάσματα εμφανίζονται ως φακοειδή ή στρωματόμορφα σώματα ή ως φλέβες. Τα εν λόγω κοιτάσματα σχετίζονται με ηφαιστειακή δραστηριότητα σε τάφρο ηφαιστειακού τόξου στα περιθώρια μιας παλαιό-ηπειρού. Στους οφιόλιθους διεισδύουν χαλαζιακές αριστερόστροφες φλέβες με B- έως BBA-κατευθύνσεις που πληρώνονται με γαλακτόχρωμο χαλαζία-σιδηροπυρίτη-ασβεσίτη. Τις χαλαζιακές φλέβες συνοδεύουν ζώνες εξαλλοίωσης από γαλακτόχρωμο χαλαζία-ασβεσίτη, αλβίτη-σερικίτη-χλωρίτη, και χαλκηδόνιο-επίδοτο-αργιλικά ορυκτά. Η Te-

μεταλλοφορία αναπτύσσεται σε δύο ακόλουθα στάδια που χαρακτηρίζονται από τις παραγενέσεις: σιδηροπυρίτης-(μαγνητοπυρίτης)-μαγνητίτης-χαλκοπυρίτης-σφαλερίτης (Στάδιο I) και γαληνίτης-σφαλερίτης-φρεϊβεργίτης-μαρκασίτης-χαλκοσύνης (Στάδιο II). Η εφαρμογή του γεωθερμομέτρου κοβαλιούχου σιδηροπυρίτη-χαλκοπυρίτη καθόρισε δύο θερμοκρασιακά πεδία εξισορρόπησης της μεταλλοφορίας στους 220°-250°C (Στάδιο I) και 120°-195°C (Στάδιο II) (Skounakis and Sovatzoglou-Skounaki, 1981). Οι υπολογιζόμενες ισοτοπικές τιμές  $\delta^{18}\text{O}$  και  $\delta\text{D}$  στους 200° και 250°C υποδεικνύουν μαγματική προέλευση του μεταλλοφόρου ρευστού. Οι υπολογιζόμενες τιμές  $\delta^{34}\text{S}_{\text{H}_2\text{S}}$  αποκαλύπτουν μαγματική πηγή για το θείο, με μικρή συνεισφορά από τα υποθαλάσσια ιζήματα που καλύπτουν τους οφιόλιθους, ενώ το τελλούριο προτείνεται ότι προέρχεται από βασική-υπερβασική μαγματική πηγή.

**Λέξεις κλειδιά:** Cu-Te σιδηροπυρίτης, οφιόλιθοι, Μειοκαινικής ηλικίας τάφρος ηφαιστειακού τόξου, κοιτάσματα Ερμιόνης-Αργολίδα.

## 1. Introduction

Cupriferous tellurium-bearing pyrite mineralization at Hermione, Argolis, Hellas, was first recognized by Aronis (1951) and Voreadis (1958). Pyrite was used for the production of sulfuric acid. The pyrite ores consists of irregularly lenticular to stratiform ore bodies, formed due to hydrothermal development in ocean floor. Ferro-manganese formations accompany the pyrite ores, and they are interpreted as submarine hydrothermal exhalations (Varnavas and Panagos 1989). In this study, a detailed investigation of mineralogical, paragenetic and stable isotope (S, O, and H) characteristics have been conducted to constrain the provenance of the mineralizing fluids, sulfur and tellurium.

## 2. Geological Setting

### 2.1. Tectonic Stratigraphy

The geology of Argolis consists of a carbonate platform of Upper Triassic neritic limestones, as well as, the Middle Jurassic Ammonitico Rosso formation (Fig. 1a) (Dostal *et al.* 1991, Saccani *et al.* 1991, 2004, Tsikouras *et al.* 1989). There is a transitional zone of iron formations which in Hermione is about 5 m wide. This is overlain by the ophiolites which consist of massive metabasalts, overlain by pillow lavas, and cut by diabase dykes representing the lava feeders (Robertson *et al.* 1991). This unit is overlain by an ophiolitic mélange with blocks of harzburgites, dunites, pyroxenites, gabbros, pillowed lavas, and thin tectonically interleaved massive sulphide ores. The sequence is tectonically overlain by Paleocene-Eocene thick flysch and pelagic manganiferous sedimentary rocks (Clift and Robertson 1990, Clift and Dixon 1998, Robertson *et al.* 1991).

At Hermione overlying the Trapezonian carbonate platform, a section of shales interbedded with sandstones is interleaved with pillow lavas, iron formations and pyrite ores (Marinos 1953, 1955, Sideris and Skounakis 1987, Sideris *et al.* 1987) (Fig. 1b). This formation is overlain by turbidite sandstones, limited shales, and conglomerates. The area of Hermione is characterized by a conjugate system of N-trending sinistral and W-trending dextral strike-slip faults and anticlines with axes of NNE and WNW directions, respectively (Doutsos *et al.* 1993).

### 2.2. Palimpsest Assemblages and Grade of Metamorphism of Host Ophiolites

The peridotites, when locally preserved consist of olivine (vol. > 85 %), ortho- and clinopyroxene, and magnetite, with secondary serpentine and quartz. Dunites, pyroxenites and peridotites are usually transformed to serpentinites with 70-85 % vol. serpentine, total primary and secondary magnetite vol. 5-10 %, relict olivine, and ortho- and clinopyroxene (Hatzipanagiotou *et al.* 1988, Tsikouras *et al.* 1989). The palimpsest assemblage in the basalts consist of labradorite

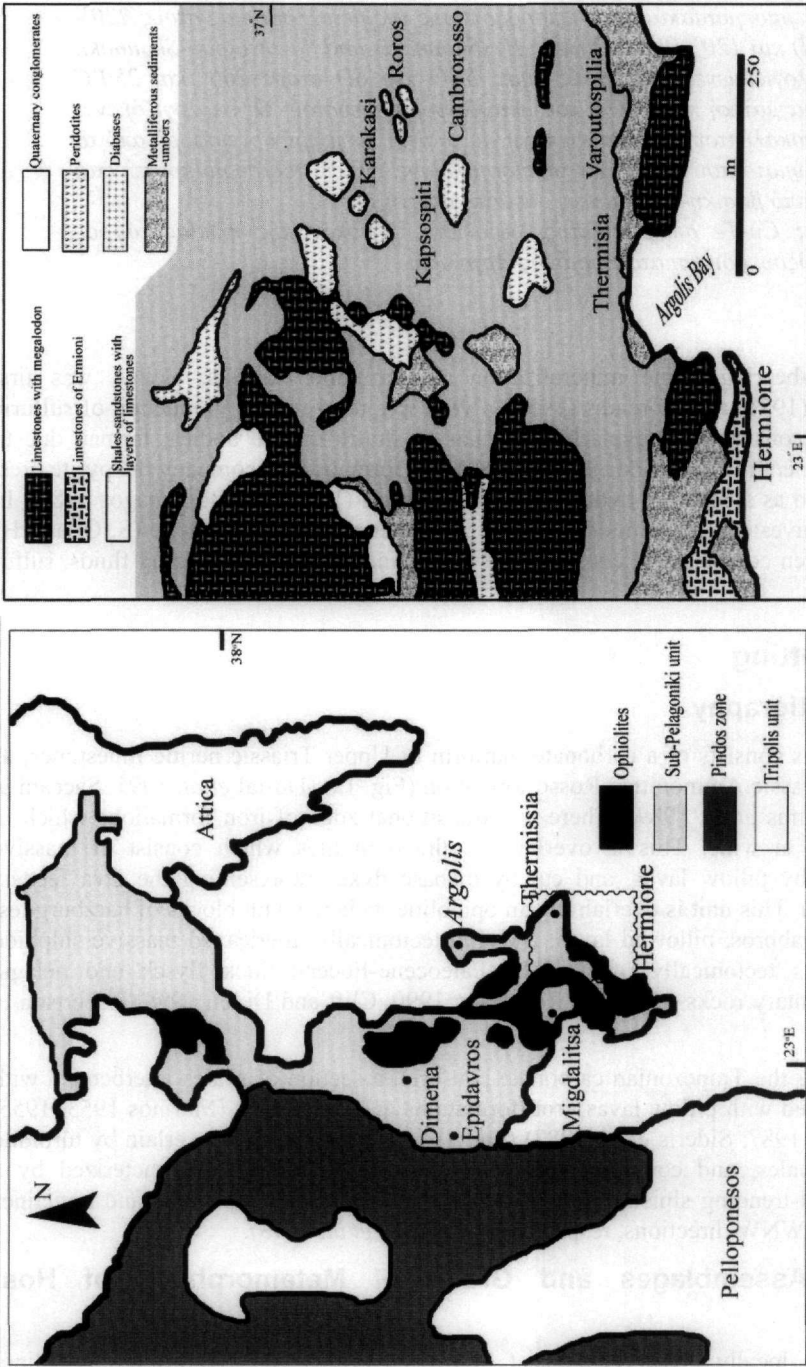


Figure 1 - a. Map showing generalized geology of Argolis, with emphasis on the ophiolite complex and the location of Hermione (modified after Dostal *et al.* 1991, Clift and Dixon 1998). 1b. Map showing generalized geology and ore deposits of Hermione (modified after Aronis 1951, Marinos 1953, 1955, Voreadis 1958, Varnavas and Panagos 1989) (The square in Figure 1a represents the studied area of Figure 1b).

(vol.  $\leq 50$  %), augite (vol.  $\leq 30$  %), olivine (vol.  $\leq 10$  %), magnetite and ilmenite; by the relict primary assemblage andesine, hornblende, biotite and clinopyroxene, whilst the diabase dykes consist of phenocrystals of labradorite (vol.  $\leq 45$  %), and metamorphosed glass. The glass is metamorphosed to chlorite, epidote, calcite, quartz and albite. Olivines and orthopyroxenes are replaced by serpentine, subordinate chlorite and secondary magnetite. Clinopyroxenes are replaced by epidote, chlorite and calcite; Primary plagioclases by more sodic plagioclase (anorthoclase, albite), calcite, and epidote (Saccani *et al.* 1991, Clift and Dixon 1998). All these secondary assemblages indicate low grade metamorphism/rock-seawater interaction in the low greenschist facies ( $P \approx 2.5$  kbars and  $T = 200-300$  °C). The andesites are characterized by the assemblage andesine ( $An_{40-47}$ ), biotite, hornblende, quartz, diopside and minor albite (Dostal *et al.* 1991).

### 3. Materials and Methods

Compositions of Hermione ore minerals were determined with a JOEL 8900 Superprobe, equipped with wave and energy dispersive and back-scattered capabilities at the Microprobe Center of the Department of Earth and Planetary Sciences, at McGill University, Montréal, Canada. Operating conditions were an accelerating voltage of 15 kV, a beam current of 10 nA and counting times of 20 sec. Standards used were natural chalcopyrite, pyrite, sphalerite, galena and native Ag, Sb, Au, Se, Cd, and Te. The X-ray lines measured were Ag *La*, Sb *La*, Cd *La*, Cu *Ka*, Fe *Ka*, Au *Ma*, Mn *Ka*, Se *La*, Ta *La*, Te *La* and S *Ka*. ZAF corrections were made with proprietary JOEL software. A minimum of 5 analyses, in grain traverses, were obtained from each sample.

Material for stable isotope studies was obtained from vein calcite and quartz, host basalts and diabase lavas and pyrite, chalcopyrite, sphalerite and galena. All minerals selected were handpicked and checked under a binocular microscope to ensure a purity of  $> 95$  %. Isotopic compositions of oxygen, hydrogen and carbon were analyzed on a VGSIRA12 triple collector mass spectrometer and those of sulfur with a VGMM602E double collector mass spectrometer. The analyses were performed at Stable Isotope Laboratory, Department of Geological Sciences, Indiana University. Oxygen was released from quartz and muscovite using the  $BrF_5$  extraction technique of Clayton and Mayeda, (1963). Sulfur was released as  $SO_2$  by heating samples to  $1.100^\circ C$  in the presence of CuO (Fritz *et al.* 1974). Hydrogen in muscovite and chlorite was converted to  $H_2$  by successive passes over uranium heated to  $800^\circ C$  (Friedman and O'Neil 1977). The isotopic ratios are reported in standard  $\delta$  notation per mil relative to SMOW for oxygen and hydrogen, Pee Dee belemnite for carbon, and Cañon Diablo troilite for sulfur. Analytical precision was better than  $\pm 0.1$  per mil for  $\delta^{18}O$  and  $\delta^{13}C$ ,  $\pm 1$  per mil for  $\delta D$ , and  $\pm 0.2$  per mil for  $\delta^{34}S$ .

Trace element analyses were obtained from ACT Labs (Canada). Major element compositions were obtained by X-ray fluorescence analysis following the method of Taggart *et al.* (1987). Trace element compositions were measured by inductively coupled plasma atomic emission spectrometry (ICP) and inductively coupled plasma mass spectrometry (ICP-MS) using the technique of Meier *et al.* (1994), whereas Te and Au was analyzed by flame atomic absorption (Hubert and Chao 1985). Trace element data were collected from samples of massive pyrite and chalcopyrite ores, calcite-quartz veins, and host lavas.

### 4. Ore Deposits

In Hermione copper-bearing pyrite deposits are located at Karakasi, Roros and Camborosso (Fig. 1b). Most of the deposits occur as veins within the blocks of peridotite as veins in the lavas, as lenses at lava tops, and as lenses and layers within the tuffs and tuffaceous iron formations overlying the lavas. In the latter case a 2-6 m layer of red iron formation cover the pyrite ores. Manganese deposits with the assemblage pyrolusite, quartz, hematite, with minor clays and K-feldspars are associated with the pyrite ores at Roros and Camborosso.

Exploration in the Karakasi mines revealed the presence of two mainly chalcopyrite lenses with northeasterly trending axes and dimensions of 8 x 80 m and 5 x 56 m, respectively (Aronis 1951, Voreadis 1958). At Roros, the ore deposits consist of 5 x 30 m, and a few smaller lenses. Pyrite at the uppermost part is altered to limonite. Locally the deposits are overlain by ochre and ferromanganiferous umbers, which are enriched in Fe, Mn, Cu, Zn, Ni, Co and Pb (Varnavas and Panagos 1984). Usually the ore deposits lie directly on the lavas; however, rarely occur as replacement of calcareous sandstones and limestones due to *remobilization*. The diabases in the area form a conjugate system of NW-, WNW- and NE-trending veins, with widths  $\leq 50$  m. Late N- to NNA-trending dextral veins of milky quartz, calcite, oligoclase ( $An_{16-18}$ ) and pyrite, with widths of  $> 0.5$  m, accompanied by networks of veinlets, intrude the hosts, or even the ores, and mainly in the contacts with the ore bodies.

## 5. Ore Mineralogy, Textures and Ore Chemistry

At Hermione Cu-bearing pyrite ores display two ore mineral assemblages characterized by different degrees of deformation and re-equilibration temperatures, which are followed by a supergene stage (Table 1). *Assemblage-(Stage) I* is characterized by subhedral pyrite (pyritohedra up to 1.5 cm in length) in intimately intergrown with pyrrhotite and minor subhedral magnetite, chalcopyrite and sphalerite. The pyrite is intensely brecciated, and cemented by quartz, calcite, sphalerite and chalcopyrite. It also appears as disseminations in the quartz veins. Pyrite contains Cu up to 2.39 wt. % (0.04 *apfu*), Zn up to 0.12 wt. %, Au up to 0.03 wt. %, Co up to 0.24 wt. %, Te up to 0.56 wt. % (0.04 *apfu*), As up to 0.13 wt. % and Se up to 0.02 wt. % (Tables 2, 3). In *Assemblage-(Stage) II* the pyrite is more intensely brecciated, veined and cemented by abundant chalcopyrite. Minor galena, sphalerite freibergite  $[(Ag,Cu,Fe)_{12}(Sb,As)_4S_{13}]$  characterize this assemblage, as well as, chalcocite which can reach up to 25 % vol. Soft minerals such as chalcopyrite, galena, freibergite and chalcocite vein and replace the pyrite along fractures, cleavage planes and crystal rims. Marcasite is present as replacement of pyrrhotite. Chalcopyrite contains Te up to 0.29 wt. % (0.01 *apfu*), whereas sphalerite bears Cd up to 0.39 wt. % (Table 2). The iron content in sphalerite ranges from 2.53 to 7.82 wt. %, corresponding to 4.4 to 14.93 mol % FeS (Table 2). Supergene stage consists of covellite, idaite, limonite, melantirite  $[Fe_2(SO_4)_3]$ , malachite and azurite.

According to Skounakis and Sovatzoglou-Skounaki (1975, 1981) the less deformed pyrite ores yields higher temperatures of equilibration (220°-250 °C) than the intensely deformed pyrite-chalcopyrite pair (120°-195 °C). These re-equilibration temperatures are inferior to the maximum temperatures of deposition of a pyrite-chalcopyrite ore in mid-ocean black smokers, which reaches  $\approx 375$  °C. The pressure of fluid entrapment was calculated from the thicknesses of the overlying shale-sandstone formation rock column, which at Hermione area is estimated to be  $\approx 1.7$  km (Aronis 1951, Marinos 1953, 1955, Paraskevopoulos 1969). This corresponds to a lithostatic pressure of 450 bars or a hydrostatic pressure of 165 bars.

## 6. Hydrothermal Alteration

Alteration haloes develop around barren and mineralized milky quartz-calcite veins and at the contacts of the ore lenses with the hosts. They form discontinuous borders and shells (Aronis 1951). Alteration consists of three zones: an inner milky quartz-calcite zone, an intermediate albite-sericite-chlorite zone and an outer dictite-illite-smectite zone. Milky quartz-calcite zones are up to 25 cm wide and contain fine-grained (0.1-1.5 mm) milky quartz, calcite, oligoclase and minor pyrite. The albite-sericite-chlorite zones have widths up to 15 cm and comprise of minor milky quartz, sericite, albite, chlorite and pyrite. The outer haloes contain chalcedony, epidote, kaoline, dickite, illite, smectite, hematite, Fe-, Mn- and Cu- oxides and hydroxides (with Mn  $\approx 41$  wt. %, Varnavas and Panagos 1984).



**Table 1 - Ore paragenesis from Karakasi mines, Hermione**

<b>Mineral stages</b>	<b>Stage I</b>	<b>Stage II</b>	<b>Stage III</b>
<i>T</i> (°C)	250-220	195-120	<100
Milky Qtz	████████	████████	
Calcite	████████	████████	
Chlorite	████	████	
Muscovite	████	████	
Albite	████	████	
Epidote		██	
Pyrite	████████	████	
Pyrrhotite	██	██	
Magnetite	██	██	
Chalcopyrite	██	████	
Sphalerite	██	████	
Marcasite	██	████████	
Galena		██	
Freibergite		██	
Chalcocite		██	
Azurite			████
Malachite			████
Covellite			████
Idaite			████
Hematite			████
Meladerite			████
Meladerite			████

## 7. Pressure-Temperature Conditions of Ore Equilibration

Since cobalt is a trace element in both pyrite and chalcopyrite, of the Hermione ores, Skounakis and Sovatzoglou-Skounaki (1975, 1981) defined two temperature intervals for the last equilibration of the Hermione ores using a geothermometer based on cobalt partitioning between co-existing pyrite and chalcopyrite (Benzen 1978). These two temperature intervals correspond to deformed (120° to 195 °C) versus less-deformed (220° to 250 °C) pyrite and chalcopyrite ores (Skounakis and Sovatzoglou-Skounaki 1975, 1981).

Pressure of last-equilibration of the Hermione ores can be estimated using the sphalerite geobarometer (Scott and Barnes 1971, Scott, 1973, Hutchinson and Scott 1981). The change in the amount of FeS in sphalerite with increasing pressure along the vertical attitude of the sphalerite-pyrite-hexagonal pyrrhotite volvus can be used as a geobarometer. This assumes that sphalerite is a refractory mineral that does not re-equilibrate during cooling, and that minor amounts of other elements i.e., Cu and Cb in sphalerite do not affect its function. Sphalerites in Hermione ores display zonation with respect to FeS, Cu and to a lesser degree in Cb contents. Cores are low in

Table 2 - Representative electron microprobe analyses of major ore minerals from Karakasi mines, Hermione

Mineral	1	1	1	1	1	1	1	1	1	1	1	1	1	1	1	1	1	1	1	1	2	2	2	3	3		
Ag	0.01	0.01	0.00	0.00	0.00	0.00	0.00	0.00	0.00	0.00	0.00	0.00	0.00	0.00	0.00	0.00	0.00	0.00	0.00	0.00	0.00	0.00	0.00	0.00	0.00	0.00	
Cu	0.05	0.00	0.03	0.02	0.04	0.00	0.02	0.04	0.00	0.02	0.00	0.00	0.00	0.00	0.00	0.00	0.00	0.00	0.00	0.00	0.00	0.00	0.00	0.00	0.00	0.00	
Zn	0.00	0.03	0.04	0.00	0.12	0.00	0.01	0.00	0.00	0.00	0.00	0.00	0.00	0.00	0.00	0.00	0.00	0.00	0.00	0.00	0.00	0.00	0.00	0.00	0.00	0.00	
Au	0.00	0.02	0.01	0.00	0.00	0.00	0.01	0.00	0.00	0.00	0.00	0.00	0.00	0.00	0.00	0.00	0.00	0.00	0.00	0.00	0.00	0.00	0.00	0.00	0.00	0.00	
Ni	0.00	0.00	0.20	0.01	0.03	0.00	0.03	0.00	0.00	0.00	0.00	0.00	0.00	0.00	0.00	0.00	0.00	0.00	0.00	0.00	0.00	0.00	0.00	0.00	0.00	0.00	
Fe	46.58	46.51	46.15	45.98	46.31	46.26	46.28	45.90	46.20	46.39	46.27	45.01	29.66	30.15	7.82	0.00	0.00	0.00	0.00	0.00	0.00	0.00	0.00	0.00	0.00	0.00	0.00
Sr	0.00	0.00	0.03	0.00	0.01	0.02	0.02	0.00	0.00	0.00	0.00	0.00	0.00	0.00	0.00	0.00	0.00	0.00	0.00	0.00	0.00	0.00	0.00	0.00	0.00	0.00	
Ba	0.00	0.00	0.00	0.00	0.00	0.00	0.00	0.00	0.00	0.00	0.00	0.00	0.00	0.00	0.00	0.00	0.00	0.00	0.00	0.00	0.00	0.00	0.00	0.00	0.00	0.00	
Co	0.00	0.00	0.00	0.24	0.03	0.03	0.22	0.07	0.00	0.00	0.00	0.00	0.00	0.00	0.00	0.00	0.00	0.00	0.00	0.00	0.00	0.00	0.00	0.00	0.00	0.00	
Cb	0.02	0.02	0.02	0.03	0.02	0.03	0.02	0.02	0.01	0.02	0.01	0.00	0.00	0.00	0.00	0.00	0.00	0.00	0.00	0.00	0.00	0.00	0.00	0.00	0.00	0.00	
Te	0.01	0.01	0.02	0.00	0.00	0.00	0.00	0.00	0.00	0.00	0.00	0.00	0.00	0.00	0.00	0.00	0.00	0.00	0.00	0.00	0.00	0.00	0.00	0.00	0.00	0.00	
As	0.00	0.02	0.01	0.00	0.13	0.00	0.00	0.00	0.00	0.00	0.00	0.00	0.00	0.00	0.00	0.00	0.00	0.00	0.00	0.00	0.00	0.00	0.00	0.00	0.00	0.00	
Sb	0.00	0.00	0.00	0.00	0.00	0.00	0.00	0.00	0.00	0.00	0.00	0.00	0.00	0.00	0.00	0.00	0.00	0.00	0.00	0.00	0.00	0.00	0.00	0.00	0.00	0.00	
Se	0.00	0.01	0.02	0.01	0.00	0.01	0.00	0.00	0.00	0.00	0.00	0.00	0.00	0.00	0.00	0.00	0.00	0.00	0.00	0.00	0.00	0.00	0.00	0.00	0.00	0.00	
S	52.60	53.100	52.91	52.74	52.29	52.90	52.96	52.23	53.093	52.603	53.33	52.303	33.62	35.19	32.64	33.654	32.64	33.654	32.64	33.654	32.64	33.654	32.64	33.654	32.64	33.654	
Total	99.29	99.73	99.79	99.04	99.00	99.33	99.53	99.33	99.34	99.10	99.21	99.164	99.59	99.41	99.43	99.43	99.43	99.43	99.43	99.43	99.43	99.43	99.43	99.43	99.43	99.43	
No of atoms																											
Ag	0.00	0.00	0.00	0.00	0.00	0.00	0.00	0.00	0.00	0.00	0.00	0.00	0.00	0.00	0.00	0.00	0.00	0.00	0.00	0.00	0.00	0.00	0.00	0.00	0.00	0.00	0.00
Cu	0.00	0.00	0.00	0.00	0.00	0.00	0.00	0.01 <sup>d</sup>	0.00	0.00	0.00	0.00	0.00	0.00	0.00	0.00	0.00	0.00	0.00	0.00	0.00	0.00	0.00	0.00	0.00	0.00	
Zn	0.00	0.00	0.00	0.00	0.01 <sup>c</sup>	0.00	0.00	0.00	0.00	0.00	0.00	0.00	0.00	0.00	0.00	0.00	0.00	0.00	0.00	0.00	0.00	0.00	0.00	0.00	0.00	0.00	
Au	0.00	0.00	0.00	0.00	0.00	0.00	0.00	0.00	0.00	0.00	0.00	0.00	0.00	0.00	0.00	0.00	0.00	0.00	0.00	0.00	0.00	0.00	0.00	0.00	0.00	0.00	
Ni	0.00	0.00	0.01 <sup>a</sup>	0.00	0.00	0.00	0.00	0.00	0.00	0.00	0.00	0.00	0.00	0.00	0.00	0.00	0.00	0.00	0.00	0.00	0.00	0.00	0.00	0.00	0.00	0.00	
Fe	1.00	1.00	0.99 <sup>a</sup>	0.99 <sup>b</sup>	0.99 <sup>c</sup>	1.00	1.00	0.99 <sup>d</sup>	1.00	1.00	1.00	0.98 <sup>d</sup>	0.41	0.41	0.05 <sup>e</sup>	0.13 <sup>g</sup>	0.00	0.00	0.00	0.00	0.00	0.00	0.00	0.00	0.00	0.00	0.00
Sr	0.00	0.00	0.00	0.00	0.00	0.00	0.00	0.00	0.00	0.00	0.00	0.00	0.00	0.00	0.00	0.00	0.00	0.00	0.00	0.00	0.00	0.00	0.00	0.00	0.00	0.00	
Ba	0.00	0.00	0.00	0.00	0.00	0.00	0.00	0.00	0.00	0.00	0.00	0.00	0.00	0.00	0.00	0.00	0.00	0.00	0.00	0.00	0.00	0.00	0.00	0.00	0.00	0.00	
Co	0.00	0.00	0.00	0.01 <sup>b</sup>	0.00	0.00	0.00	0.00	0.00	0.00	0.00	0.00	0.00	0.00	0.00	0.00	0.00	0.00	0.00	0.00	0.00	0.00	0.00	0.00	0.00	0.00	
Cb	0.00	0.00	0.00	0.00	0.00	0.00	0.00	0.00	0.00	0.00	0.00	0.00	0.00	0.00	0.00	0.00	0.00	0.00	0.00	0.00	0.00	0.00	0.00	0.00	0.00	0.00	
Te	0.00	0.00	0.00	0.00	0.00	0.00	0.00	0.00	0.00	0.00	0.00	0.00	0.00	0.00	0.00	0.00	0.00	0.00	0.00	0.00	0.00	0.00	0.00	0.00	0.00	0.00	
Sb	0.00	0.00	0.00	0.00	0.00	0.00	0.00	0.00	0.00	0.00	0.00	0.00	0.00	0.00	0.00	0.00	0.00	0.00	0.00	0.00	0.00	0.00	0.00	0.00	0.00	0.00	
As	0.00	0.00	0.00	0.00	0.01 <sup>e</sup>	0.00	0.00	0.00	0.00	0.00	0.00	0.00	0.00	0.00	0.00	0.00	0.00	0.00	0.00	0.00	0.00	0.00	0.00	0.00	0.00	0.00	
Se	0.00	0.00	0.00	0.00	0.00	0.00	0.00	0.00	0.00	0.00	0.00	0.00	0.00	0.00	0.00	0.00	0.00	0.00	0.00	0.00	0.00	0.00	0.00	0.00	0.00	0.00	
S	2.00	2.00	2.00	2.00	1.99 <sup>e</sup>	2.00	2.00	2.00	2.00	2.00	2.00	1.99 <sup>f</sup>	2.00	2.00	2.00	2.00	2.00	2.00	2.00	2.00	2.00	2.00	2.00	2.00	2.00	2.00	
Te/Te+S	0.00	0.00	0.00	0.00	0.00	0.00	0.00	0.00	0.00	0.00	0.00	0.00	0.00	0.00	0.00	0.00	0.00	0.00	0.00	0.00	0.00	0.00	0.00	0.00	0.00		
FeS (mol %)	0.00	0.00	0.00	0.00	0.00	0.00	0.00	0.00	0.00	0.00	0.00	0.00	0.00	0.00	0.00	0.00	0.00	0.00	0.00	0.00	0.00	0.00	0.00	0.00	0.00		

Samples analysed: E<sub>3</sub>, E<sub>4</sub>.

<sup>1</sup> Pyrite from stage I

<sup>2</sup> Chalcopyrite from stage II

<sup>3</sup> Sphalerite from stage II

<sup>a</sup>Fe + Ni = 1, S = 2

<sup>b</sup>Fe + Co = 1, S = 2

<sup>c</sup>Fe + Zn = 1, S = 2

<sup>d</sup>Fe + Cu = 1, S = 2

<sup>e</sup>S + As = 1

<sup>f</sup>S + Te = 1

<sup>g</sup>Zn + Fe + Cu + Co = 1, S = 2

FeS (average  $\approx 4$  mol % FeS) (Fig. 2), Cu and to a lesser degree higher in Cb contents with respect to sphalerite mantles and periphery of the crystals which are higher in FeS (average  $\approx 15$  mol % FeS) (Fig. 2), high in Cu and somewhat lower in Cb. Due to the presence of Cu up 6.45 wt. % the results from the external portions of the sphalerite crystals were corrected before the application of the geobarometer by the method suggested by Hutchison and Scott (1981). The results of sphalerite geobarometry for the Hermione ores indicate that the cores of sphalerite crystals which are low in FeS must have formed at low pressures which probably reflect the ore formation pressures (i.e., 450 bars), whereas sphalerite mantles and rims display pressure values of equilibration of 2.5 kbars reflecting pressures of regional low grade metamorphism.

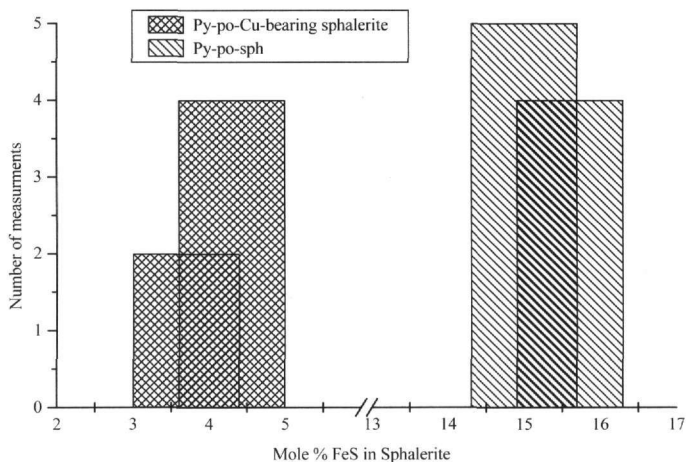


**Figure 2 - Histogram of the frequency of sphalerite compositions in the Hermione ore, distinguished by the copper content**

## 8. Stable Isotopes Studies

### 8.1. Oxygen and hydrogen isotopes

Oxygen and hydrogen isotope compositions are given in Figure 3 and were obtained from fluids released by samples of vein calcite and milky quartz, host basalts and diabase lavas and pyrite, chalcocopyrite, sphalerite and galena. The  $\delta^{18}\text{O}$  and  $\delta\text{D}$  values of chlorite and sericite from the pillow lavas range from 12.3 to 18.7 per mil and from -74.2 to -63.2 per mil, respectively. We have used the average temperatures of 200° and 250°C obtained from the Co-pyrite-chalcocopyrite geothermometer, (Skounakis and Sovatzoglou-Skounaki 1975, 1981) to calculate the fluid isotopic signature. The calculated  $\delta^{18}\text{O}$  and  $\delta\text{D}$  values of the fluid in equilibrium with these minerals are 7.9 to 9.1 per mil and -53.6 to -44.3 per mil, respectively. The  $\delta^{18}\text{O}$  and  $\delta\text{D}$  values of milky quartz veins range from 4.2 to 5.8 per mil and -72.7 to -71.1 per mil, respectively. The corresponding  $\delta^{18}\text{O}$  and  $\delta\text{D}$  values of the fluid in equilibrium with quartz are from -4.2 to -2.8 per mil and -55.1 to -54.2 per mil, respectively. The oxygen and hydrogen fluid isotopic values of vein milky quartz are approximately 6.5 and 10 per mil lighter than of those of chlorite and sericite.

### 8.2. Sulfur isotopes

Sulfur isotope compositions were obtained on samples of pyrite, chalcocopyrite, sphalerite and galena, representing Stages I and II. The  $\delta^{34}\text{S}$  values range from 0.1 for Stage II-galena to 5.3 per mil for Stage I-pyrite. The calculated  $\delta^{34}\text{S}_{\text{H}_2\text{S}}$  values for the fluid range from -3.1 to 1.2 per mil (Table 4).



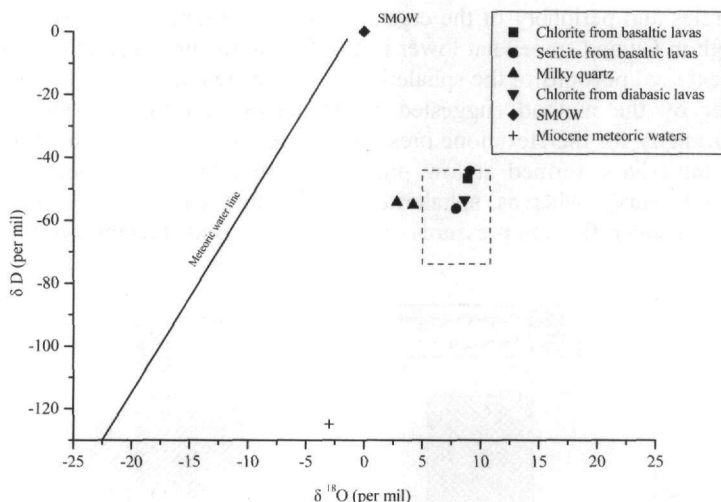


**Figure 3 - Hydrogen versus oxygen isotope diagram displaying stable calculated isotope systematics of hydrothermal fluids, at of 200° and 250 °C, from Hermione, Argolis. Dot lines refer to “Subduction-related vapor, arc and crystal felsic magma (Hedenquist and Lowenstern 1994). The calculated  $\delta O^{18}$  and  $\delta D$  mineralizing fluid values were obtained by utilizing the chlorite-water equation of Wenner and Taylor (1971); the muscovite-water equations of O’ Neil and Taylor (1972) and Suzuoki and Epstein (1976), and the quartz-water equation of Clayton *et al.* (1972)**

**Table 3 - Sulfur isotopes obtained from pyrite, chalcopyrite, sphalerite and galena, Karakasi mines, Hermione**

Sample	Mineral	$\delta S^{34}$	T °C	$\delta S^{34}_{\text{‰}}^A$
E3	1	5.3	250 <sup>B</sup>	1.2
E4	1	4.7	250 <sup>B</sup>	0.8
E8	1	4.0	250 <sup>B</sup>	0.4
E3	2	5.4	220 <sup>B</sup>	0.6
E4	2	4.3	250 <sup>B</sup>	0.5
E8	2	4.2	250 <sup>B</sup>	0.4
E3	3	0.5	220 <sup>B</sup>	-3.1
E4	4	0.9	220 <sup>B</sup>	-2.7
E8	5	0.1	220 <sup>B</sup>	-2.3

<sup>A</sup>Utilizing the H<sub>2</sub>S-sulfides equations of Ohmoto and Rye (1979) and Ohmoto and Lasaga (1982).

<sup>B</sup>Utilizing the Co-pyrite-chalcopyrite geothermometer (Skounakis and Sovatzoglou-Skounaki, 1975, 1981).

<sup>1</sup>Pyrite from stage I

<sup>3</sup>Sphalerite from stage II

<sup>5</sup>Galena from stage II

<sup>2</sup>Chalcopyrite from stage I

<sup>4</sup>Chalcopyrite from stage II

## 9. Discussion

The geometry, host rock (metamorphosed ocean floor crust) and ore assemblages of the Hermione rocks indicate a formation similar to that of mid ocean ridge black smoker ore deposits. However, the trace element contents of the host basalts indicated that they are more evolved than MORBS (Tsikouras *et al.* 1989, Dostal *et al.* 1991, Saccani *et al.* 1991), and the presence of Pb in the ores indicates hydrothermal leaching of more felsic rocks present in the volcanic pile (Table 4). The suggested depositional petrotectonic environment in a back-arc basin (Sideris *et al.* 1897), appears

**Table 4 - Representative major (wt. %) and trace (ppm) element analyses of vein and host rocks from the Karakasi mines, Hermione**

Mineral	1	2	2	3	4	5	5
SiO <sub>2</sub>	52.60	47.3	48.65	59.54	93.54	1.10	0.80
TiO <sub>2</sub>	0.01	0.65	1.37	0.45	0.02	0.07	0.06
Al <sub>2</sub> O <sub>3</sub>	18.17	16.40	16.82	15.86	0.25	0.52	0.75
Fe <sub>2</sub> O <sub>3</sub>	8.67	10.39	10.19	6.95	0.40	0.72	0.97
MgO	10.38	7.13	8.72	5.36	0.16	5.28	6.89
CaO	5.03	9.29	7.95	3.78	0.94	45.16	47.12
Na <sub>2</sub> O	0.02	3.10	3.27	6.05	0.21	0.26	0.63
K <sub>2</sub> O	0.06	0.58	0.55	0.05	1.02	0.30	0.41
P <sub>2</sub> O <sub>5</sub>	0.01	0.05	0.07	0.06	0.01	0.02	0.03
SO <sub>2</sub>	0.4	0.01	0.02	0.02	0.01	0.02	0.03
LOI	3.86	4.95	3.35	1.75	3.32	46.55	41.82
Total	99.22	99.85	99.61	99.97	99.88	99.98	99.51
Y	2	35	12	12	6	7	10
Zr	98	89	105	44	20	18	13
Cu	2220	44	51	71	43	83	575
Pb	<3	3	4	4	4	7	9
Zn	375	55	84	66	<1	28	50
Ag	<0.3	<0.3	<0.3	<0.3	<0.3	<0.3	<0.3
Br	1.8	<0.5	<0.5	<0.5	<0.5	<0.5	<0.5
Au	<2	<2	<2	<2	<2	<2	3
As	0.6	<0.5	0.5	0.7	0.6	<0.5	2.6
Co	20	29	35	12	3	15	19
Cs	<1	<1	<1	<1	<1	2	<1
Th	<0.2	<0.2	1	2	0.9	2	1.9
U	1.1	1.6	1.3	0.2	<0.5	<0.5	<0.5
Ge	<0.1	0.2	0.2	<0.1	<0.1	<0.1	<0.1
Cd	3.2	<0.3	<0.3	<0.3	<0.3	<0.3	<0.3
Ni	3	49	92	41	6	13	19
Ba	<50	160	145	28	70	<50	<50
V	4	221	298	240	8	21	21
Cr	<2	322	315	78	11	26	18
Mn	74	834	1925	1200	1630	1730	1560
Sb	<0.1	0.2	0.2	0.4	<0.1	<0.1	0.2
Sc	0.3	37	41	42	1.5	26	33
Te	2.8	0.6	0.7	0.3	3.2	3.4	2.9

Samples analysed: E4, E5, E6, E7, E8, E9, E10.

<sup>1</sup> Diabasic lavas

<sup>3</sup> Andesites

<sup>5</sup> Calcite from pyrite veins

<sup>2</sup> Basaltic pillow lavas

<sup>4</sup> Quartz from pyrite veins

therefore to be quite plausible. The ores formed at a maximum temperature of 375 °C for pyrite-chalcopyrite and at lower temperatures for sphalerite, less so galena and chalcocite but nevertheless in excess of 200 °C. The ores formed at the ocean floor but subsequently were covered by shale-sandstone turbidites and equilibrated to fluid pressures of 165 bars hydrostatic or 450 bars lithostatic corresponding to an average 1.7 km of sediments.

The enclosing volcanic hosts show metamorphic assemblages replacing palimpsest mineralogy, characteristic of low grade metamorphose of low grade i.e. low greenschist facies. The volcanic rocks have been metamorphose in a pressure-temperature framework of approximately  $P \approx 2.5$  kbars and  $T \approx 250$  °C. Sphalerite geobarometry reveals that the sphalerite external mantles and rims have also re-equilibrated at the same pressures. The ores are extremely deformed most probably during the overthrust of the tectonic slides forming breccias being cemented by the softer more plastic sulfides such as chalcopyrite, galena freibergite and chalcocite. Deformed ores have re-equilibrated to 220° to 250 °C and intensely deformed ores to 120° to 195 °C (Skounakis and Sovatzoglou-Skounaki 1975, 1981).

The calculated  $\delta^{34}\text{S}_{\text{H}_2\text{S}}$  values of the mineralizing fluids range from -3.2 to 1.4 per mil (Table 3). Stage I shows typical magmatic values of  $\delta^{34}\text{S}_{\text{H}_2\text{S}}$ , i.e. 0.3 to 1.4 per mil, respectively, whereas Stage II shows negative  $\delta^{34}\text{S}_{\text{H}_2\text{S}}$  values i.e., -3.2 and -2.4 per mil, which is consistent with minor

contribution from the submarine sediments. The presence of base metals assemblages indicates that the dominant sulfur species, in solution, was  $H_2S$  (Barnes 1979). The calculated compositions of the Hermione mineralizing fluids are shown on Figure 3 on conventional hydrogen versus oxygen isotope diagram. The isotopic compositions reflect the dominance of a magmatic component related to volcanic activity in an active arc-related rift. The lighter  $\delta^{18}O$  and  $\delta D$  values of vein milky quartz can be attributed to mixing of magmatic with seawater, and water-rock interaction.

We have no primary isotope data for the source of tellurium, however, Cooke *et al.* (1996) proposed that the presence of tellurium in epithermal gold systems is indicative of a magmatic signature to the hydrothermal fluid. Given the presence of tellurium in hydrothermal exhalations derived from MORBS it is possible that this semi-metal was derived from leaching of mantle derived rocks such as the meta-basalts and ultramafics of the ophiolites, and then partitioned in the sulphides. Tellurium re-distribution is possible to be related with release of  $CO_2$ , as documented from the vein calcite precipitation and the high fluorine contents of the magmatic fluids associated with alkaline volcanic activity in the Hermione area (Spry *et al.* 1996).

## 10. Acknowledgments

Research funds for this work were obtained from a "Pythagoras II" grant to KStS and post-doctoral fellowship to S. Tombros. We thank the European Social Fund (ESF), Operational Program for Educational and Vocational Training II (EPEAEK II), and particularly the Program PYTHAGORAS II, for funding the above work.

## 11. References

- Aronis, G., 1951. Research on the iron-pyrite deposits in the Hermione district, *I.G.M.E.*, 2, 1-35.
- Barnes, L.H., 1979. Geochemistry of hydrothermal ore deposits. In H.L. Barnes (ed.), *Special Edition, Wiley, J., and Sons inc., New York*, 800pp.
- Benzen, N.I, Yeremin, N.I., Narazauli, I.G., Pozdnyakova, N.V., and Sergeyevan, Y.E., 1978. Cobalt distribution and the pyrite-chalcopyrite geothermometer, *Geochemical International*, 15, 1-10.
- Clayton, R.N., Muffler, L.J.P., and White, D.E., 1972. Oxygen isotope fractionation study of calcite and silicates of the River Ranch, California, *American Journal of Science*, 266, 968-979.
- Clayton, R.N., and Mayeda, T.K., 1963. The use of bromine penta-fluoride in the extraction of oxygen from oxides and silicates for isotopic analysis, *Geochemica et Cosmochimica Acta*, 27, 43-52.
- Clift, P.D., and Dixon, J.E., 1998. Jurassic ridge collapse, subduction initiation and ophiolite obduction in the southern Greek Tethys, *Eclogae Geology Helvetica*, 91, 128-139.
- Clift, P.D., and Robertson, A.H.F., 1990. Deep-water basins within a Mesozoic carbonate platform, Argolis, Greece, *Journal of Geological Society of London*, 147, 825-835.
- Cooke, R., Mc Phail, D., and Bloom, M., 1996. Epithermal gold mineralization, Acupan, Baguio district, Phippines: Geology, mineralization, alteration and the thermochemical environment of ore deposition, *Economic Geology*, 94, 243-272.
- Dostal, J., Toscani, L., Photiades, A., and Capedri, S., 1991. Geochemistry and petrogenesis of Tethyan ophiolites from northern Argolis (Peloponnesus, Greece), *European Journal of Mineralogy*, 3, 105-121.
- Doutsos, T., Pe-Piper, G., Boronkay, K., and Koukouvelas, I., 1993. Kinematics of the central Hellenides, *Tectonics*, 12, 936-953.

- Friedman, I., and O'Neil, J.R., 1977. Compilation of stable isotope fractionation factors of geochemical interest, *US Geological Survey Professional Paper*, 440, 1-12.
- Fritz, P., Drimmie, R.J., and Norwick, K., 1974. Preparation of sulfur dioxide for mass spectrometer analysis by combustion of sulfide with copper oxide, *Analytical Chemistry*, 76, 164-166.
- Hatzipanagiotou, K., Tsikouras, B., and Gaitanakis, P., 1988. Study of the ophiolitic outcrops in central Argolis: Ophiolite mélange and residual ophiolitic nappe, *Annales Géologiques des Pays Helléniques*, 33, 475-492.
- Hedenquist, J.W., and Lowenstern, J.B., 1994. The role of magmas in the formation of hydrothermal ore deposits, *Nature*, 370, 519-527.
- Hubert, A.E., and Chao, T.T., 1985. Determination of gold, indium, tellurium, and thallium in the same sample digestion of geological materials by atomic-absorption spectrometry and two-step solvent extraction, *Talanta*, 32, 523-548.
- Hutchison, N.M., and Scott, D.S., 1981. Sphalerite geobarometry in the Cu-Fe-Zn-S system, *Economic Geology*, 76, 143-153.
- Marinos, G., 1955. The granitic rocks of Argolis and the age of the shale-sandstone formation, *Bulletin of Geological Society of Greece*, 1, 45-59.
- Marinos, G., 1953. Preliminary studies of the pyrite deposits of Plepi area, Ermioni, *I.G.M.E., Unpublished Essay*, 3, 100pp.
- Meier, A.L., Grimes, D.J., and Ficklin, W.H., 1994. Inductively coupled plasma mass spectrometry: A powerful analytical tool for mineral resource and environmental studies, *US Geological Survey Circular*, 1103, 67-68.
- Ohmoto, H., and Lasaga, A.C., 1982. Kinetics of reactions between aqueous sulfates and sulfides in hydrothermal systems, *Geochemica et Cosmochimica Acta*, 46, 1727-1745.
- Ohmoto, H., and Rye, R.O., 1979. Isotopes of sulfur and carbon. In H.L. Barnes (ed.), *Geochemistry of hydrothermal ore deposits*, 2<sup>nd</sup> edition, New York, Wiley Interscience, 509-567.
- O'Neil, J.R., and Taylor, H.P.Jr, 1972. Oxygen isotope fractionation between muscovite and water, *Journal of Geophysical Research*, 74, 6012-6022.
- Paraskevopoulos, G., 1969. Mineral Deposits, *University of Athens Publication*, 376pp.
- Robertson, A.H.F., Clift, P.D., Degnan, P.J., and Jones, G., 1991. Palaeogeographic and palaeotectonic evolution of the eastern Mediterranean Neotethys, *Palaeogeography, Palaeoclimatology, Palaeoecology*, 87, 289-343.
- Saccani, E., Padoa, E., and Photiades, A., 2004. Triassic mid-ocean ridge basalts from the Argolis peninsula (Greece): New constraints for the early oceanization phases of the Neo-Tethyan Pindos basin. In Y. Dilekand and P.T. Robinson (eds), *Ophiolites in earth history*, *Geological Society of London Special Publication*, 218, 109-127.
- Saccani, E., Padoa, E., and Photiades, A., 1991. Tectono-magmatic significance of Triassic MORBS from the Argolis peninsula (Greece): Implications for the origin of the Pindos ocean, *European Journal of Mineralogy*, 3, 105-121.
- Scott, S.D., 1973. Experimental calibration of the sphalerite geobarometer, *Economic Geology*, 68, 466-474.
- Scott, S.D., and Barnes, H.L., 1971. Sphalerite geothermometry and geobarometry, *Economic Geology*, 66, 653-669.

- Sideris, C., and Skounakis, S., 1987. Metallogeny in the basic rocks of a paleosubduction area: The case of Ermioni area Cu-bearing pyrite mines (East Peloponnesos, Greece), *Chemie der Erde*, 47, 93-96.
- Sideris, C., Skounakis, S., and Simantov, J., 1987. Trace and REE geochemistry of a basic lava series from the Ermioni area (Argolis peninsula) Greece, *Ofoliti*, 12, 1-107.
- Skounakis, S., and Sovatzoglou-Skounaki, E., 1975. The Co and Ni traces distribution within the deposits of Cu-bearing pyrite of Ermioni, Argolida, *Bulletin of Geological Society of Greece*, 13, 54-60.
- Skounakis, S., and Sovatzoglou-Skounaki, E., 1981. The  $\text{CuFeS}_2\text{-FeS}_2\text{-Co}$ -contribution geothermometer, within the deposits of Cu-bearing pyrite of Ermioni, Argolida and Perivoli Grevena, *Bulletin of Geological Society of Greece*, 15, 74-78.
- Spry, G.P., Paredes, M.M., Foster, F., Truckle, S.J., and Chadwick, H.T., 1996. Evidence for a genetic link between gold-silver telluride and porphyry mineralization at the Golden Sunlight Deposit, Whitehall, Montana: Fluid inclusion and stable isotopes studies, *Economic Geology*, 91, 507-526.
- Suzuoki, T., and Epstein S., 1976. Hydrogen isotope fractionation between OH-bearing minerals and water, *Geochemica et Cosmochimica Acta*, 40, 1229-1240.
- Taggart, J.E.Jr, Lindsey, J.R., Scott, B.A., Vivit, D.V., Bartel, A.J., and Stewart, K.C., 1987. Analysis of geological materials by wavelength-dispersive X-ray fluorescence spectrometry, *US Geological Survey Professional Paper*, 1770, 1-19.
- Tsikouras, B., Traki, K., Katsantouri, O., and Hatzipanagiotou, K., 1989. Contribution to geological structure and petrography of the ophiolite mélange and relict ophiolite nappe in northern Argolis, *Bulletin of Geological Society of Greece*, 13, 347-362.
- Varnavas, S.P., and Panagos, A.G., 1989. Some observations on the sulphide mineralization at the Mesozoic ocean ridge in the Hermione area, Greece, *Chemie der Erde*, 49, 81-90.
- Varnavas, S.P., and Panagos, A.G., 1984. Mesozoic metalliferous sediments from the ophiolites of Ermioni, Greece: Analogue to recent mid-ocean ridge ferromanganese deposits, *Chemical Geology*, 42, 227-242.
- Voreadis, G., 1958, Genesis of the pyrite and manganese deposits of Ermioni and their relationships, *Bulletin of Geological Society of Greece*, 3, 50-63.